



# Improved Time of Arrival measurement model for non-convex optimization

Juri Sidorenko<sup>1,2</sup> | Volker Schatz<sup>1</sup> | Leo Doktorski<sup>1</sup> | Norbert Scherer-Negenborn<sup>1</sup> | Michael Arens<sup>1</sup> | Urs Hugentobler<sup>2</sup>

<sup>1</sup>Fraunhofer Institute of Optronics, System Technologies and Image Exploitation IOSB, Ettlingen, Germany

<sup>2</sup>Institute of Astronomical and Physical Geodesy, Technical University of Munich, Munich, Germany

## Correspondence

Juri Sidorenko, Fraunhofer Institute of Optronics, System Technologies and Image Exploitation IOSB, Ettlingen, Germany.  
Email: juri.sidorenko@iosb.fraunhofer.de

## Funding information

Fraunhofer IOSB

## Abstract

The quadratic system provided by the Time of Arrival technique can be solved analytically or by nonlinear least squares minimization. An important problem in quadratic optimization is the possible convergence to a local minimum, instead of the global minimum. This problem does not occur for Global Navigation Satellite Systems (GNSS), due to the known satellite positions. In applications with unknown positions of the reference stations, such as indoor localization with self-calibration, local minima are an important issue. This article presents an approach showing how this risk can be significantly reduced. The main idea of our approach is to transform the local minimum to a saddle point by increasing the number of dimensions. In addition to numerical tests, we analytically prove the theorem and the criteria that no other local minima exist for nontrivial constellations.

## 1 | INTRODUCTION

In position estimation, the Time of Arrival (ToA)<sup>1</sup> technique is standard. The area of applications extends from satellite-based systems like GPS,<sup>2</sup> GLONASS,<sup>3</sup> Galileo,<sup>4</sup> mobile phone localization (GSM),<sup>5</sup> and radar-based systems such as UWB<sup>6</sup> and FMCW radar<sup>7</sup> to acoustic systems.<sup>8</sup>

The ToA technique leads to a quadratic equation. Optimization algorithms used to solve this system depend on the initial estimate. Unfortunately chosen initial estimates can cause the optimization algorithm to converge to the local minimum. With known reference station positions, it is possible to transform the quadratic to a linear system.<sup>9-11</sup> This linear system can be used to provide an initial estimate. On the other hand, the linear system is more affected by noise, compared with the quadratic system.<sup>9,10</sup> In general, local minima are not an issue in

applications with known reference station positions such as GNSS. This changes if it is necessary to obtain the locations of the reference stations without additional measuring equipment, which is also known as self-calibration. The most robust self-calibration solution with noise is nonlinear optimization.<sup>12</sup> This solution suffers if the initial estimates are not close to the global minimum.<sup>13-15</sup> In Mekonnen and Wittneben<sup>16</sup> and Biswas et al,<sup>17</sup> it was proposed to use semi-definite relaxation (SDP) as an initialization for the maximum likelihood (ML) estimator. Nuclear norm-based methods<sup>18-20</sup> also reduce the risk of being trapped in a local minimum. Alternatively, non-iterative methods can be used. A two-dimensional non-iterative method was proposed for the case with three transponders and three receivers in Stewénius.<sup>21</sup> The solution for the three-dimensional case was the subject of the investigation in Kuang<sup>22</sup> and Pollefeys and Nister.<sup>23</sup> The authors

This is an open access article under the terms of the Creative Commons Attribution-NonCommercial License, which permits use, distribution and reproduction in any medium, provided the original work is properly cited and is not used for commercial purposes.

© 2019 Fraunhofer IOSB. *Journal of the Institute of Navigation* published by Wiley Periodicals, Inc. on behalf of Institute of Navigation

provided a non-iterative solution for the cases with (5, 5), (6,4), and (10,4) transponders and receivers. The roles of the base stations and the transponders are equivalent; hence, it does not matter if six base stations and four transponders are used or vice versa. In the case that one of the base station positions coincides with the position of one of the transponders, it is possible to obtain a closed form solution.<sup>24,25</sup> An alternative approach is called far field.<sup>26</sup> If the distances between the base stations and the transponders are considerably larger than those between the base stations, it is also possible to use a linear simplification. Real measurement data are highly non-convex and nonlinear optimization still provides the most robust solutions.<sup>12</sup>

We present a new approach which does not require an initial estimate at all. The idea is that an additional dimension in the  $l^2$  norm transforms the local minimum of the ToA equation to a saddle point without adding more local minima. This is not equivalent to a receiver time offset, which would be added or subtracted outside the norm. Under the constraint that the position of the reference stations is known, we prove that with our approach, the local minimum becomes a saddle point and no further local minima exist for nontrivial constellations. This paper focuses on proving our approach. Further publications will be based on this concept and will investigate its practical use for self-calibration.

Our approach is based on introducing an additional dimension. It can be seen as a kind of lifting method, a generic term covering many numerical methods introducing an additional variable. Lifting methods have been used for solving nonlinear optimization problems,<sup>27</sup> machine learning problems,<sup>28</sup> optimal control problems,<sup>29</sup> boundary value problems,<sup>30</sup> and parameter estimation problems in ordinary differential equations (ODE).<sup>31</sup> To the best of our knowledge, our specific approach has not been applied before, in particular in the context of ToA localization. It does not work with every objective function, but we will show that it is suitable for ToA localization equations.

This paper is organized as follows. The next section introduces the objective functions  $F$  and the corresponding improved objective functions  $F_L$ . In Section 3, we use the Levenberg-Marquardt algorithm<sup>32</sup> to illustrate the optimization steps for  $F$  and  $F_L$ . The last section addresses the results of the optimization algorithm with randomly selected constellations.

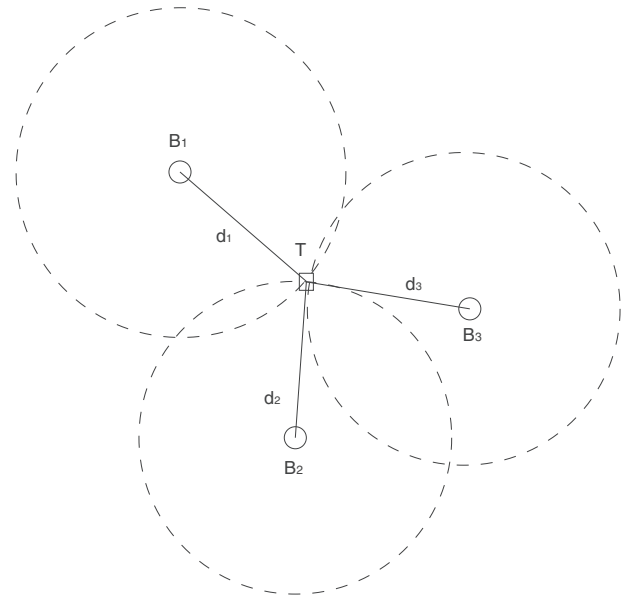
## 2 | METHODOLOGY

Table 1 provides notations used throughout this paper.

Figure 1 shows three base stations  $B_i$  at known positions  $(a_i, b_i, c_i)$  and one object  $T$  at unknown position  $(x, y, z)$ . The distance measurements  $d_i$  between base stations  $B_i$

**TABLE 1** Used notations

Notations	Definition
$x, y, z$	Estimated position of object $T$
$x_G, y_G, z_G$	Ground truth position of object $T$
$a_i, b_i, c_i$	Ground truth position of base stations $B_i, 1 \leq i \leq N$
$d_i$	Distance measurements between base stations $B_i$ and object $T$
$\lambda$	Additional variable



**FIGURE 1** The dashed circles are the distances between the base stations  $B_i$  and object  $T$ . The object  $T$  is located at the intersection point between the three dashed circles

and object  $T$  are known and derived from time of flight measurements. The unknown position of object  $T$  can be estimated by the known positions of the base stations  $B_i$  and the distance measurements  $d_i$ . Measurement errors are neglected in this paper; therefore, distance measurements can be referred to as distances.

### 2.1 | Mathematical formulation

The distances between the base station  $B_i$  and object  $T$  are defined as follows:

$$d_i^2 = (x_G - a_i)^2 + (y_G - b_i)^2 + (z_G - c_i)^2, \quad 1 \leq i \leq N.$$

- Objective function  $F_1$ :

$$F_1(x, y, z) := \frac{1}{4} \sum_{i=1}^N \left[ \sqrt{(x-a_i)^2 + (y-b_i)^2 + (z-c_i)^2} - d_i \right]^2 \quad (1)$$

- Objective function  $F_2$ :

$$F_2(x, y, z) := \frac{1}{4} \sum_{i=1}^N [(x - a_i)^2 + (y - b_i)^2 + (z - c_i)^2 - d_i^2]^2. \quad (2)$$

(see Douglass<sup>2</sup> and Thompson<sup>33</sup>). Finding the minimum of the objective function of (1) or (2) can be done by non-convex optimization.<sup>34</sup> Alternatively, the nonlinear system can be transformed into a linear system.<sup>9,10</sup> With the assumptions made in Section 2.1, it is possible to obtain a linear system. With regard to future extensions to determining the base station positions as well as the location of the object  $T$ , this article focuses on finding a solution with a non-convex optimization algorithm.

## 2.2 | Reason for the approach

The objective functions (1) and (2) are nonlinear and non-convex. Numerical optimization can cause convergence to a local minimum  $L$  instead of the global minimum  $G$ . In our approach, instead of  $F_1$  (1) and  $F_2$  (2), the improved objective functions  $F_{L1}$  and  $F_{L2}$  are used. Both have an additional variable  $\lambda$  compared with the  $F$  functions.

- Improved objective function  $F_{L1}$ :

$$F_{L1}(x, y, z, \lambda) := \frac{1}{4} \sum_{i=1}^N \left[ \sqrt{(x - a_i)^2 + (y - b_i)^2 + (z - c_i)^2 + \lambda^2} - d_i \right]^2. \quad (3)$$

- Improved objective function  $F_{L2}$ :

$$F_{L2}(x, y, z, \lambda) := \frac{1}{4} \sum_{i=1}^N [(x - a_i)^2 + (y - b_i)^2 + (z - c_i)^2 + \lambda^2 - d_i^2]^2. \quad (4)$$

In the next section, we prove that  $F_{L2}$  (4) has a saddle point at every position of the local minimum  $L(x_L, y_L, z_L)$  of  $F_2$  (2). Therefore, the Levenberg-Marquardt algorithm has a lower probability of converging to a local minimum. The additional variable  $\lambda$  is not equivalent to a receiver time offset in GNSS, which would be added or subtracted outside the norm.

## 2.3 | Characteristics of a local minimum

### 2.3.1 | Assumption

The objective function has a unique global minimum at  $G(x_G, y_G, z_G)$  and at least one local minimum at  $L(x_L, y_L, z_L)$ .

### 2.3.2 | Criterion

It is known that the first derivative of  $F_L$  with respect to  $x$ ,  $y$ , and  $z$  is zero at the local minimum. The criterion is that the second derivative of  $F_L$  at the same position is positive (Table 2).

## 2.4 | Assertion

The first derivative of  $F_L$  with respect to the additional variable  $\lambda$  is zero, and the second derivative is less than zero at the local minimum (Table 3). In combination with the assumption and the criterion, the local minimum becomes a saddle point. The Levenberg-Marquardt (derivative-based optimization algorithm) would not converge to a saddle point.

### 2.4.1 | Assertion for function $F_1$

Every local minimum of function  $F_1$  (1) becomes a saddle point at the same coordinates with function  $F_{L1}$  (3). We have no analytical proof of this assertion, but the numerical results in Section 3 demonstrate its validity in practice.

### 2.4.2 | Assertion for function $F_2$

Every local minimum of function  $F_2$  (2) becomes a saddle point at the same coordinates with function  $F_{L2}$  (4). This assertion is proven analytically in Appendix A and demonstrated numerically in Section 3.

TABLE 2 Criterion

First Derivative	Second Derivative
$\left(\frac{\partial}{\partial x} F_L\right)(x_L, y_L, z_L, 0) = 0$	$\left(\frac{\partial^2}{\partial x^2} F_L\right)(x_L, y_L, z_L, 0) > 0$
$\left(\frac{\partial}{\partial y} F_L\right)(x_L, y_L, z_L, 0) = 0$	$\left(\frac{\partial^2}{\partial y^2} F_L\right)(x_L, y_L, z_L, 0) > 0$
$\left(\frac{\partial}{\partial z} F_L\right)(x_L, y_L, z_L, 0) = 0$	$\left(\frac{\partial^2}{\partial z^2} F_L\right)(x_L, y_L, z_L, 0) > 0$

TABLE 3 Assertions of our approach

First Derivative	Second Derivative
$\left(\frac{\partial}{\partial \lambda} F_L\right)(x_L, y_L, z_L, 0) = 0$	$\left(\frac{\partial^2}{\partial \lambda^2} F_L\right)(x_L, y_L, z_L, 0) < 0$
	$\left(\frac{\partial^2}{\partial x \partial \lambda} F_L\right)(x_L, y_L, z_L, 0) = 0$
	$\left(\frac{\partial^2}{\partial y \partial \lambda} F_L\right)(x_L, y_L, z_L, 0) = 0$
	$\left(\frac{\partial^2}{\partial z \partial \lambda} F_L\right)(x_L, y_L, z_L, 0) = 0$

## 2.5 | The effect of an additional variable on the global minimum

At the global minimum, the additional variable  $\lambda$  must be zero, and the second derivative must be positive. The second derivative of  $F_{L2}$  (4) with respect to  $\lambda$  at the global minimum is the following:

$$\left(\frac{\partial^2}{\partial \lambda^2} F_{L2}\right)(x_G, y_G, z_G, \lambda_G) = 3\lambda_G^2 N = 0.$$

If the second derivative is zero, a higher-order derivative is required.

$$\left(\frac{\partial^3}{\partial \lambda^3} F_{L2}\right)(x_G, y_G, z_G, \lambda_G) = \sum_{i=1}^N 6\lambda_G N = 0.$$

The third derivative is also zero. Finally, the fourth derivative is greater than zero; hence, the additional variable has no effect on the global minimum.

$$\left(\frac{\partial^4}{\partial \lambda^4} F_{L2}\right)(x_G, y_G, z_G, \lambda_G) = 6N.$$

## 2.6 | No new local minima for $F_{L2}$ with $\lambda \neq 0$

We have shown that the modified objective function  $F_{L2}$  (4) turns the local minima of  $F_2$  (2) into saddle points and leaves the global minimum unaffected. It must still be proven that  $F_{L2}$  does not introduce new local minima that might adversely affect convergence to the global minimum.

In this section, we will show that in practically relevant base station arrangements,  $F_{L2}$  has no stationary points for  $\lambda \neq 0$  and  $\mathbf{x} \neq \mathbf{x}_G$ , and therefore, no minima that would lead an optimization method astray. We will show that if the first derivative of  $F_{L2}$  with respect to  $\lambda$  vanishes when  $\lambda \neq 0$ , its gradient in the spatial directions is nonzero for  $\mathbf{x} \neq \mathbf{x}_G$ . This proof is best presented in vectorial notation. We will use  $\mathbf{x} = (x, y, z)^T$  for the position argument and  $\mathbf{a}_i = (a_i, b_i, c_i)^T$  for the base station locations.

$$\begin{aligned} \frac{\partial}{\partial \lambda} F_{L2}(\mathbf{x}, \lambda) &= \lambda \sum_i ((\mathbf{x} - \mathbf{a}_i)^2 + \lambda^2 - d_i^2) = 0, \quad \lambda \neq 0 \\ &\Rightarrow \sum_i ((\mathbf{x} - \mathbf{a}_i)^2 + \lambda^2 - d_i^2) = 0, \end{aligned} \quad (5)$$

$$\text{grad}_{\mathbf{x}} F_{L2}(\mathbf{x}, \lambda) = \sum_i ((\mathbf{x} - \mathbf{a}_i)^2 + \lambda^2 - d_i^2) (\mathbf{x} - \mathbf{a}_i). \quad (6)$$

Equation 5 allows us to add or subtract any term not dependent on the summation index  $i$  in the right-hand factor of (6). We subtract  $\mathbf{x}$  and add  $\mathbf{a}_* = \frac{1}{N} \sum_{i=1}^N \mathbf{a}_i$ , the geometrical center of the base stations:

$$\begin{aligned} \text{grad}_{\mathbf{x}} F_{L2}(\mathbf{x}, \lambda) &= \sum_i ((\mathbf{x} - \mathbf{a}_i)^2 + \lambda^2 - d_i^2) (\mathbf{x} - \mathbf{a}_i - \mathbf{x} + \mathbf{a}_*) \\ &= - \sum_i ((\mathbf{x} - \mathbf{a}_i)^2 + \lambda^2 - d_i^2) (\mathbf{a}_i - \mathbf{a}_*). \end{aligned}$$

By the construction of  $\mathbf{a}_*$ , we have  $\sum_{i=1}^N (\mathbf{a}_i - \mathbf{a}_*) = 0$ , so now we can add or subtract any term not depending on the summation index in the left-hand factor. We add  $-\lambda^2 - \mathbf{x}^2 + \mathbf{x}_G^2$  and substitute  $d_i = |\mathbf{x}_G - \mathbf{a}_i|$ , expand the squares and simplify, obtaining the following:

$$\begin{aligned} \text{grad}_{\mathbf{x}} F_{L2}(\mathbf{x}, \lambda) &= - \sum_i ((\mathbf{x} - \mathbf{a}_i)^2 - \mathbf{x}^2 + \mathbf{x}_G^2 - d_i^2) (\mathbf{a}_i - \mathbf{a}_*) \\ &= - \sum_i ((\mathbf{x} - \mathbf{a}_i)^2 - \mathbf{x}^2 + \mathbf{x}_G^2 - (\mathbf{x}_G - \mathbf{a}_i)^2) \\ &\quad (\mathbf{a}_i - \mathbf{a}_*) \\ &= \sum_i (2\mathbf{x}\mathbf{a}_i - 2\mathbf{x}_G\mathbf{a}_i) (\mathbf{a}_i - \mathbf{a}_*) \\ &= 2(\mathbf{x} - \mathbf{x}_G)^T \sum_i \mathbf{a}_i \otimes (\mathbf{a}_i - \mathbf{a}_*) \\ &= 2(\mathbf{x} - \mathbf{x}_G)^T \mathbf{M}. \end{aligned}$$

Here,  $\mathbf{u} \otimes \mathbf{v}$  denotes the outer product, resulting in a matrix with the entries  $u_i v_j$ . The matrix  $\mathbf{M}$  can be expressed in the following form:

$$\begin{aligned} \mathbf{M} &= \sum_i \mathbf{a}_i \otimes \mathbf{a}_i - \left( \sum_i \mathbf{a}_i \right) \otimes \mathbf{a}_* = \sum_i \mathbf{a}_i \otimes \mathbf{a}_i - N \mathbf{a}_* \otimes \mathbf{a}_* \\ &= \sum_i (\mathbf{a}_i - \mathbf{a}_*) \otimes (\mathbf{a}_i - \mathbf{a}_*). \end{aligned}$$

The last step is analogous to the well-known derivation of the variance of a data set. The result represents  $\mathbf{M}$  as a sum of unnormalized projection matrices onto the directions to the base stations from their center.

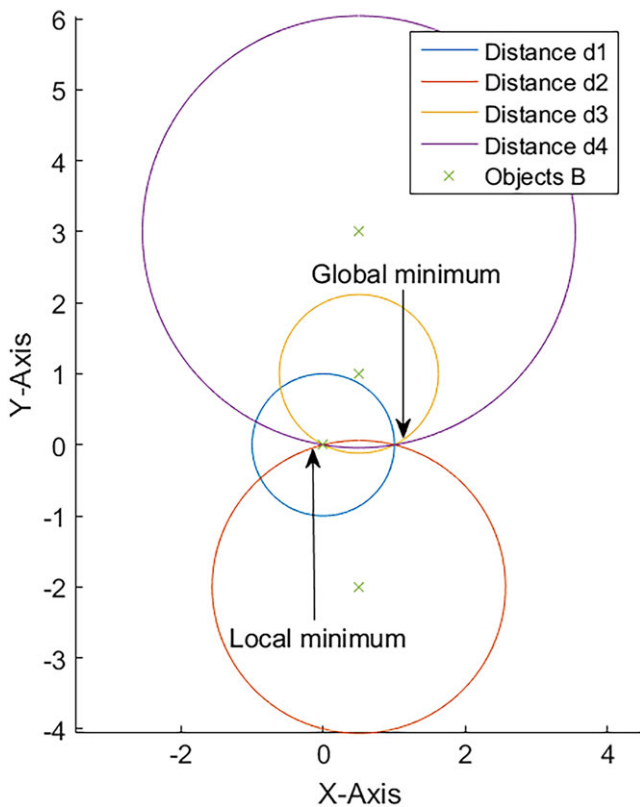
The calculation above shows that the gradient of  $F_{L2}$  has the form of a vector times a sum of projection matrices at all local minima with  $\lambda \neq 0$ . Projection matrices are positive semidefinite by construction, and their null space is the subspace orthogonal to the projection direction. When adding several positive semidefinite matrices, the null space of the result is the intersection of the null spaces of the individual matrices, in our case the subspace orthogonal to all projection directions. For unambiguous location in  $n$  (2 or 3) dimensions, at least  $n + 1$  base stations are needed, and they must be arranged in a nondegenerate way, ie, so that the  $\mathbf{a}_i - \mathbf{a}_*$  are a spanning set of the whole space. This makes the matrix  $\mathbf{M}$  positive definite, and the gradient of  $F_{L2}$  cannot be zero for  $\mathbf{x} \neq \mathbf{x}_G$ . Therefore, there are no local minima that prevent an optimization method from converging to the global minimum.

## 2.7 | Two-dimensional example

In Appendix A, it is proven that the  $F_{L2}$  (4) has a saddle point at the coordinates of the local minimum of  $F_2$  (2). In this section, an example is created with known coordinates of the global  $G(1, 0)$  and local minimum  $L(0, 0)$ . The aim of this example is to illustrate the converging steps of the

Levenberg-Marquardt algorithm for  $F_2$  and  $F_{L2}$ . The positions of the local minimum and global minimum leads to the coordinates of base stations  $B_i$  (see Table A3).

Figure 2 shows a top view perspective of the base stations  $B_i$  and object  $T$  positions inside a Cartesian coordinate system. The circles represent the distance measurements between the base stations  $B_i$  and the object  $T$ . In this example, the measurements are not corrupted by noise; hence, the ground truth position of object  $T$  is located at the intersection point between all circles. Nonlinear optimization algorithms can find the ground truth by minimizing the residues of the predefined objective function to obtain the global minimum. Under certain constellations of the base station, it is possible that the objective function used has a global minimum in addition to at least one local minimum. A more detailed description of the requirements for this kind of constellation can be found in the Appendix A.3. The local and global minima both have the commonality that the first derivative is zero and the second derivative is higher than zero. This attribute makes the local minimum a trap for derivative-based nonlinear optimization algorithms. In this example, the local minimum is located at  $L(0, 0)$  and the global minimum at  $G(1, 0)$ .



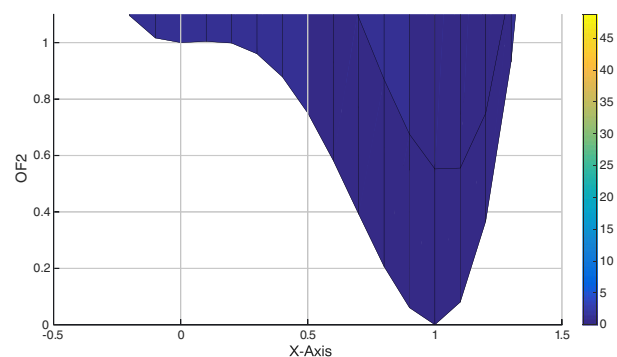
**FIGURE 2** The circles represent the true distance between base stations  $B_i$  and the global minimum. The blue, red, yellow, and magenta circles are the distances between base stations  $B$  and object  $T$ , respectively [Color figure can be viewed at [wileyonlinelibrary.com](http://wileyonlinelibrary.com) and [www.ion.org](http://www.ion.org)]

Figure 3 shows the search space of objective function  $F_2$  (2) and the zoom at the global minimum. The x-axis of Figure 3 is equivalent to the x-axis in Figure 2 and the y-axis represents the result of objective function  $F_2$ . It can be observed that the first derivative is zero, and the second derivative is higher than zero for the local minimum  $L(0, 0)$  and the global minimum  $G(1, 0)$ . The only difference between both minima is the result of the objective function. At the ground truth position  $G(1, 0)$ , the result of the objective function is zero and at the local minimum  $L(0, 0)$  it equates to one. In the case of bad initial estimates, close to the local minimum, it is possible that the derivative-based nonlinear optimization algorithm converges to the local minimum and remains there. The main aspect of our approach is to transform this local minimum to a saddle point and eliminate this trap.

### 2.7.1 | Local optimization

The Levenberg-Marquardt algorithm uses the derivative to obtain the stepsize; therefore, it is important that the initial estimate for the additional variable  $\lambda$  is nonzero. Otherwise,  $\lambda$  remains zero, and  $F_{L2}$  (4) is effectively reduced to  $F_2$  (2). The initial estimates for the optimization are  $x = -1$ ,  $y = 2$  and  $\lambda = 1$ .

Figure 4 is equivalent to Figure 2. The x-y axes represent the positions of the base stations  $B_i$  and object  $T$  inside a Cartesian coordinate system. The circles are the two-dimensional euclidean distances between the base stations  $B_i$  and object  $T$ . The main difference between Figures 2 and 4 is the additional dimension  $\lambda$  with the initial estimate one. The stepsize of the optimization algorithm is obtained by the first derivative of the objective function. The first derivative for the additional dimension at  $\lambda = 0$  is always zero and leads to a stepsize with the value zero. 
$$\left(\frac{\partial}{\partial \lambda} F_2\right)(x, y, z) = \sum_{i=1}^N [(x - a_i)^2 + (y - b_i)^2 + \lambda^2 - d_i^2] \lambda.$$



**FIGURE 3** The Local minimum is at  $L(0, 0)$  and global minimum at  $G(1, 0)$ . Colors ranging from blue to yellow show the residues of the objective function [Color figure can be viewed at [wileyonlinelibrary.com](http://wileyonlinelibrary.com) and [www.ion.org](http://www.ion.org)]

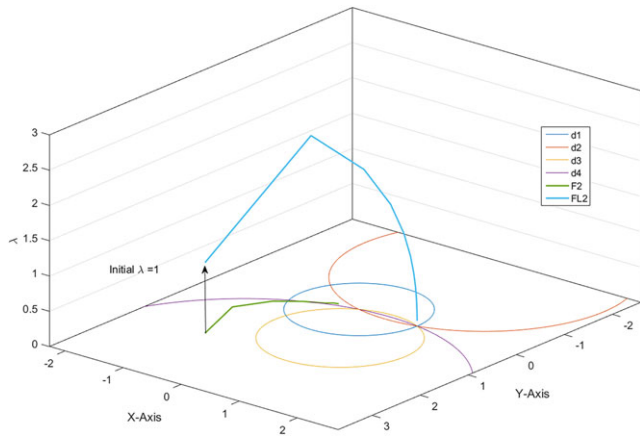


**FIGURE 4** Iteration steps of the Levenberg-Marquardt algorithm for  $F_2$  and  $F_{L2}$ .  $F_2$ : Objective function  $F_2$ .  $FL_2$ : Improved objective function  $F_{L2}$ . Blue line: Optimization steps of  $F_2$ . Green line: Optimization steps of  $F_{L2}$ . The circles blue, red, yellow and magenta are the distances between base stations  $B_i$  and object  $T$  [Color figure can be viewed at [wileyonlinelibrary.com](http://wileyonlinelibrary.com) and [www.ion.org](http://www.ion.org)]

Without using the additional dimension, the nonlinear optimization algorithm converges to the local minimum  $L(0, 0)$ . On the other hand, if the improved objective function  $F_{L2}$  is used, the same optimization algorithm converges to the global minimum  $G(1, 0)$ . The optimization steps with objective function  $F_2$  are represented by the green line and, for the improved objective function  $F_{L2}$ , by the blue line. It can be seen that the improved objective function  $F_{L2}$  allows the optimization algorithm to use the additional dimension of freedom to bypass the local minimum.

Figure 5 is divided in to two plots. Both plots are based on the same coordinate system as Figure 2, with the same positions for base stations  $B_i$ , object  $T$ , the local  $L(0, 0)$  and global minimum  $G(1, 0)$ . The colored lines represent the optimization steps. Blue lines indicate the convergence to the local minimum and the green lines to the global minimum. In the left plot, it can be observed that the correct convergence for the objective function  $F_2$  highly depends on the initial estimate of the x-coordinate. With an initial estimate  $x > 0$ , the optimization algorithm converges to the global minimum, otherwise to the local minimum. In the right plot, the improved objective function  $F_{L2}$  is used. At this point, the initial estimates for the x axis are not relevant anymore. The optimization algorithm always converges to the global minimum  $G(1, 0)$  if the initial estimate for the additional dimension  $\lambda$  is not equal to zero.

### 3 | NUMERICAL RESULTS

The base stations  $B_i$ , object  $T$  and initial estimates were randomly generated by the MATLAB “randn()” function.

This function provides normally distributed random numbers in a predefined range. This range was limited to a  $10 \times 10 \times 10$  cube. Randomly generated base station positions have the risk of creating collinear constellations with two solutions. These constellations have been avoided by considering the normalized singular value of the covariance matrix. These values provide information about how spread out the base stations are relative to each other. The threshold used for the normalized singular value was set to 0.1. Constellations with a higher value were rejected. The quality of the result is evaluated by the euclidean distance between the fitted value  $x_F, y_F$  and  $z_F$  and the ground truth position  $x_G, y_G$ , and  $z_G$ .

- Error term:

$$E = \sqrt{(x_F - x_G)^2 + (y_F - y_G)^2 + (z_F - z_G)^2}. \quad (7)$$

The tests were carried out with the MATLAB Levenberg-Marquardt algorithm using the default settings (Table 4).

#### 3.1 | Results with the objective function $F_1$ and $F_{L1}$

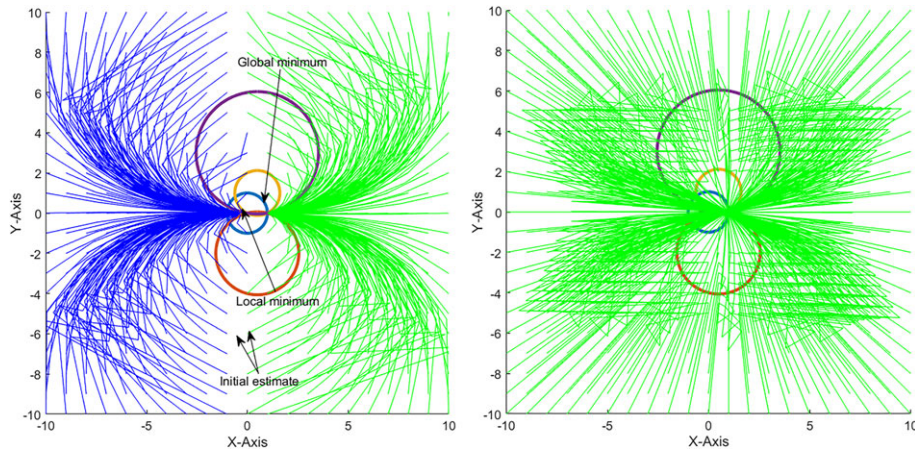
In the following section, the results of the optimization with a two-dimensional  $F_1$  and  $F_{L1}$  are presented.

Figure 6 shows the error term with different constellations of the four base stations  $B_i$  ( $N = 4$ ). The x-axis indicates the number of tests carried out. Every scenario was done with random constellations and random initial estimates. The y-axis represents the error term (7). The blue dots are the error with the objective function  $F_1$  and the red dots the improved objective function  $F_{L1}$ . It can be seen that  $F_{L1}$  has no outlier. It has yet to be proven that the local minimum of  $F_1$  becomes a saddle point for  $F_{L1}$ . However, the results show a significant effect of the  $F_{L1}$  on the optimization process.

#### 3.2 | Results with the objective function $F_2$ and $F_{L2}$

In the following section, the results of the optimization with a two-dimensional  $F_2$  and  $F_{L2}$  are presented.

Figure 7 has the same axis notations as Figure 6. The x-axis indicates the number of tests carried out and the y-axis the error term (7). The main difference from Figure 6 is that the blue dots now indicate the error with objective function  $F_2$  and the red dots the improved objective function  $F_{L2}$ . In this case, it was proven that the local minimum of  $F_2$  becomes a saddle point with an additional variable. This fact is also underpinned by the error term of  $F_{L2}$ , which is always less than 0.5.



**FIGURE 5** Left figure shows  $F_2$  and the right figure shows  $F_{L2}$  with different initial estimates. Green: Convergence to global minimum. Blue: Convergence to local minimum [Color figure can be viewed at [wileyonlinelibrary.com](http://wileyonlinelibrary.com) and [www.ion.org](http://www.ion.org)]

**TABLE 4** Default MATLAB “Levenberg Marquardt algorithm” parameters

	Value
Maximum change in variables for finite-difference gradients	Inf
Minimum change in variables for finite-difference gradients	0
Termination tolerance on the function value	1e-6
Maximum number of function evaluations allowed	100*numberOfVariables
Maximum number of iterations allowed	400
Termination tolerance on the first-order optimality	1e-4
Termination tolerance on x	1e-6
Initial value of the Levenberg-Marquardt parameter	1e-2

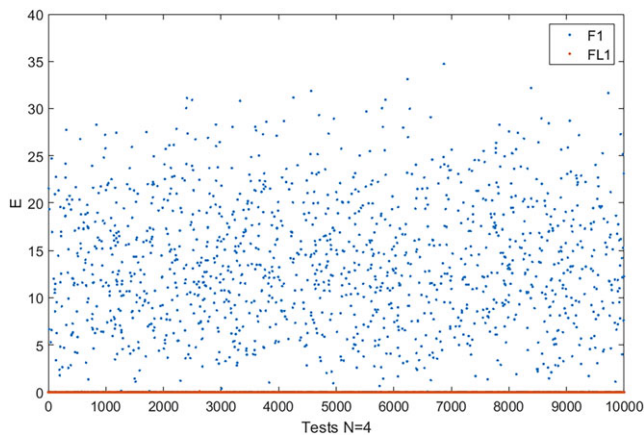


**FIGURE 6** Blue dots: Objective function  $F_1$ . Red dots: Improved objective function  $F_{L1}$  [Color figure can be viewed at [wileyonlinelibrary.com](http://wileyonlinelibrary.com) and [www.ion.org](http://www.ion.org)]

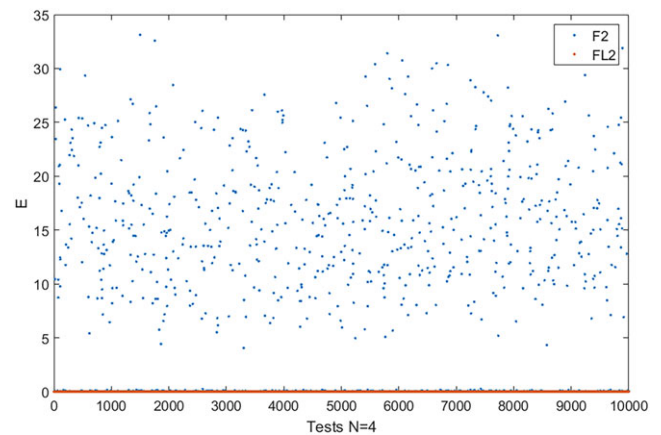


**FIGURE 7** The blue dots are the results of the error term of  $F_2$ . The red dots are the results of  $F_{L2}$  [Color figure can be viewed at [wileyonlinelibrary.com](http://wileyonlinelibrary.com) and [www.ion.org](http://www.ion.org)]

### 3.3 | Summary of the results

Tables 5 and 6 summarize the obtained results. For each number of objects ( $N$ ), 10 000 constellations have been created and tested with Levenberg-Marquardt.  $F_L$  never

converges to a local minimum. It can be observed that the risk to converge to a local minimum is decreasing for the objective function  $F_1$  and  $F_2$  with higher number of base stations. This is probably due to the increase in the convergence radius with a higher amount of base stations.

**TABLE 5** Examples are based on a 2-D model<sup>a</sup>

N	Objective Function	$F_1$ : L	$F_2$ : L
4	$F$	1357	634
4	$F_L$	0	0
5	$F$	982	399
5	$F_L$	0	0
6	$F$	810	286
6	$F_L$	0	0
7	$F$	586	182
7	$F_L$	0	0

<sup>a</sup>N, number of base stations  $B_i$ ;  $F_1$ , objective function one;  $F_2$ , objective function two; L, number of convergences to local minima (Error greater than 0.5).

**TABLE 6** Examples are based on a 3-D model<sup>a</sup>

N	Objective function	$F_1$ : L	$F_2$ : L
7	$F$	494	216
7	$F_L$	0	0

<sup>a</sup>N, number of base stations  $B_i$ ;  $F_1$ , objective function one;  $F_2$ , objective function two; L, number of convergences to local minima (Error greater than 0.5).

## 4 | CONCLUSIONS

In the Section 2, it was proven that the improved objective function  $F_{L2}$  has no local minima for nontrivial constellations. In addition to the mathematical proof, a simple two-dimensional example was created with one local minimum and one global minimum. This example illustrates how the optimization algorithm uses the additional dimension to bypass the local minimum and converges to the global minimum. This was underpinned by more than 100 000 numerical tests with reasonable constellations. It still has to be proven that the local minimum of  $F_1$  becomes a saddle point with  $F_{L1}$ . However, the results show a significant effect of  $F_{L1}$  on the optimization process. The objective function  $F_2$  performed better than the objective function  $F_1$ . Furthermore, the number of false results  $L$  decreases with a higher number of base stations  $B_i$ .

## 5 | DISCUSSION

It is important that the initial estimate of the additional variable is not equal to zero. Otherwise, gradient-based optimization algorithms like Levenberg-Marquardt would not converge to the additional dimension. This is due to the fact that the optimization algorithm used is estimating the stepsize for every dimension by the first derivative of the objective function. With  $\lambda = 0$ , the derivatives for this additional dimension are always zero; thus, the stepsize also equals zero. The test scenarios were carried out with at

least four base stations. This is due to the fact that the additional dimension requires one more measurement. In all test scenarios, the positions of base stations  $B_i$  were known. Under the condition that the reference stations are known, it is also possible to obtain the solution analytically. In the case of unknown positions of base stations  $B_i$  and objects  $T_j$ , with real measurements it is no longer feasible. At this point, our approach becomes extremely valuable.

## ACKNOWLEDGMENTS

The first author would like to thank Sebastian Bullinger, Gregor Stachowiak, and Sebastian Tome for their inspiring discussion and the Fraunhofer IOSB for making this work possible. We would also like to thank the reviewers and the Editor for their helpful and constructive comments that greatly contributed to improving the paper.

## ORCID

Juri Sidorenko  <https://orcid.org/0000-0003-0089-967X>

## REFERENCES

1. Adamy DL. *Ew 102: A Second Course in Electronic Warfare*. Boston London: Artech House; 2004.
2. Douglass D. *GPS instant navigation: a practical guide from basics to advanced techniques* by Kevin Monahan. Fine Edge Productions; 1998; Guildford.
3. Bogdanov PP, Druzhin AV, Tiuliakov AE, Feoktistov AY. GLONASS time and UTC(SU). *2014 31st URSI General Assembly and Scientific Symposium (URSI GASS)*; August 2014; Beijing:1-3.
4. Benevides P, Nico G, Catalão J, Miranda PMA. Analysis of galileo and GPS integration for GNSS tomography. *IEEE Trans Geosci Remote Sens*. April 2017;55(4):1936-1943.
5. Nambiar V, Vattapparamban E, Yurekli AI, Güvenç İ, Mozaffari M, Saad W. SDR based indoor localization using ambient WiFi and GSM signals. *2017 International Conference on Computing, Networking and Communications (ICNC)*; January 2017; Santa Clara:952-957.
6. Marquez A, Tank B, Meghani SK, Ahmed S, Tepe K. Accurate UWB and IMU based indoor localization for autonomous robots. *2017 IEEE 30th Canadian Conference on Electrical and Computer Engineering (CCECE)*; April 2017; Windsor:1-4.
7. Vossiek M, Roskosch R, Heide P. Precise 3-d object position tracking using FMCW radar. *1999 29th European Microwave Conference*, Vol. 1; October 1999; Munich:234-237.
8. Akiyama T, Sugimoto M, Hashizume H. Light-synchronized acoustic ToA measurement system for mobile smart nodes. *2014 International Conference On Indoor Positioning And Indoor Navigation (IPIN)*; October 2014; Busan:749-752.
9. Sidorenko J, Scherer-Negenborn N, Arens M, Michaelsen E. Improved linear direct solution for asynchronous radio network localization (RNL). *ION 2017 Pacific PNT*; May 2017; Honolulu, Hawaii:376-382.
10. Sidorenko J, Scherer-Negenborn N, Arens M, Michaelsen E. Multilateration of the local position measurement. *2016 International Conference on Indoor Positioning and Indoor Navigation (IPIN)*; October 2016; Alcalá de Henares:1-8.



11. Hmam H. Quadratic optimisation with one quadratic equality constraint. Electronic Warfare and Radar Division, Edinburgh, South Australia; 2010.
12. Batstone K, Oskarsson M, Åström K. Robust time-of-arrival self calibration with missing data and outliers. *2016 24th European Signal Processing Conference (EUSIPCO)*; August 2016; Budapest:2370-2374.
13. Birchfield ST, Subramanya A. Microphone array position calibration by basis-point classical multidimensional scaling. *IEEE Trans Speech Audio Process*. September 2005;13(5):1025-1034.
14. Raykar VC, Kozintsev IV, Lienhart R. Position calibration of microphones and loudspeakers in distributed computing platforms. *IEEE Trans Speech Audio Process*. January 2005;13(1):70-83.
15. Prieto J, Bahillo A, Mazuelas S, Fernández P, Lorenzo RM, Abril EJ. Self-calibration of TOA/distance relationship for wireless localization in harsh environments. *2012 IEEE International Conference On Communications (ICC)*; June 2012; Ottawa:571-575.
16. Mekonnen ZW, Wittneben A. Self-calibration method for toa based localization systems with generic synchronization requirement. *2015 IEEE International Conference On Communications (ICC)*; June 2015; London:4618-4623.
17. Biswas P, Lian T-C, Wang T-C, Ye Y. Semidefinite programming based algorithms for sensor network localization. *ACM Trans Sen Netw*. May 2006;2(2):188-220.
18. Candès EJ, Li X, Ma Y, Wright J. Robust principal component analysis. *J ACM*. June 2011;58(3):11:1-11:37.
19. Garg R, Roussos A, Agapito L. Dense variational reconstruction of non-rigid surfaces from monocular video. *2013 IEEE Conference On Computer Vision And Pattern Recognition*; June 2013; Portland:1272-1279.
20. Olsson C, Oskarsson M. A convex approach to low rank matrix approximation with missing data. *Proceedings of the 16th Scandinavian Conference on Image Analysis, SCIA '09*. Berlin, Heidelberg: Springer-Verlag; 2009:301-309.
21. Stewénius H. Gröbner Basis Methods for Minimal Problems in Computervision. *Ph.D. Thesis*: Lund Inst. for Technology, Centre for Mathematical Sciences, Lund Univ.; April 2005.
22. Kuang Y, Burgess S, Torstensson A, Åström K. A complete characterization and solution to the microphone position self-calibration problem. *2013 IEEE International Conference on Acoustics, Speech and Signal Processing*; May 2013; Vancouver:3875-3879.
23. Pollefeys M, Nister D. Direct computation of sound and microphone locations from time-difference-of-arrival data. *2008 IEEE International Conference on Acoustics, Speech and Signal Processing*; March 2008; Las Vegas:2445-2448.
24. Crocco M, Bue AD, Murino V. A bilinear approach to the position self-calibration of multiple sensors. *IEEE Trans Signal Process*. February 2012;60(2):660-673.
25. Crocco M, Bue AD, Bustreo M, Murino V. A closed form solution to the microphone position self-calibration problem. *2012 IEEE International Conference on Acoustics, Speech and Signal Processing (ICASSP)*; March 2012; Kyoto:2597-2600.
26. Kuang Y, Ask E, Burgess S, Åström K. Understanding TOA and TDOA network calibration using far field approximation as initial estimate. *International Conference on Pattern Recognition Applications And Methods*; 2012:590-596.
27. Matei I, Baras JS. Nonlinear programming methods for distributed optimization. Cornell University Library *arXiv:1707.04598*. 2017; Osaka.
28. Brafman RI, Engel Y. *Lifted optimization for relational preference rules*. Leuven, Belgium: ILP-MLG-SRL; 2009.
29. Bock HG, Plitt KJ. A multiple shooting algorithm for direct solution of optimal control problems. *9th IFAC World Congress: A Bride between control science and technology, Budapest, Hungary. IFAC Proceedings*, July 1984;17(2):1603-1608.
30. Osborne MR. On shooting methods for boundary value problems. *J Math Anal Appl*. 1969;27(2):417-433.
31. Peifer M, Timmer J. Parameter estimation in ordinary differential equations for biochemical processes using the method of multiple shooting. *IET Syst Biol*. March 2007;1(2):78-88.
32. Moré J. The Levenberg-Marquardt Algorithm: Implementation and Theory. *In Numerical Analysis*. Berlin, Heidelberg: Springer; 1978:105-116.
33. Thompson RB. Global positioning system: the mathematics of GPS receivers. *Math Mag*. 1998;71:260-269.
34. Stigler SM. Gauss and the invention of least squares. *Ann Stat*. May 1981;9(3):465-474.
35. Bityutskov VI. Bunyakovskii inequality. *Encyclopedia of Mathematics*. NY, USA: Springer, New York; 2001.

**How to cite this article:** Sidorenko J, Schatz V, Doktorski L, Scherer-Negenborn N, Arens M, Hugentobler U. Improved Time of Arrival measurement model for non-convex optimization. *NAVIGATION*. 2019;66:117-128. <https://doi.org/10.1002/navi.277>

## APPENDIX A: PROOF OF THE ASSERTION FOR OBJECTIVE FUNCTION $F_2$

In Section 2.3, the assumption and the criterion was introduced. In this section, the assertion will be proven for the objective function  $F_2$  (2). The proof of the assertion for objective function  $F_1$  (1) has yet to be found. The empirical results show that the approach works for both objective functions. First, a new coordinate system is defined. This coordinate system is centered at the local minimum with global minimum on the positive  $x$ -axis.

### A.1 | Definition of the new coordinate system

Without loss of generality, the following coordinate system can be used

$$y_G = z_G = x_L = y_L = z_L = 0,$$

and

$$x_G > 0.$$

The distances between the base stations  $B_i$  and object  $T$  are defined in Section 2.1. With the new coordinate system the equation becomes

$$d_i^2 = (x_G - a_i)^2 + (b_i)^2 + (c_i)^2.$$

The second objective function can also be written as follows:

$$F_2(x, y, z) = \sum_{i=1}^N \varphi_i(x, y, z)^2,$$

with the auxiliary function  $\varphi_i(x, y, z)$

$$\varphi_i(x, y, z) := (x - a_i)^2 + (y - b_i)^2 + (z - c_i)^2 - d_i^2.$$

At the position of the local minimum  $L$ , the auxiliary function becomes

$$\begin{aligned} \varphi_i(0, 0, 0) &= [a_i^2 + b_i^2 + c_i^2 - d_i^2] = \\ &= [a_i^2 + b_i^2 + c_i^2 - (x_G - a_i)^2 - b_i^2 - c_i^2] = \\ &= [a_i^2 - (x_G - a_i)^2] = [2a_i x_G - (x_G)^2] = x_G [2a_i - x_G]. \end{aligned} \quad (\text{A1})$$

Therefore, the second objective function at the local minimum can be written as follows:

$$F_2(0, 0, 0) = x_G^2 \sum_{i=1}^N [2a_i - x_G]^2. \quad (\text{A2})$$

In Section 2.3, the assumption and the criterion for the approach were presented.

$$\left( \frac{\partial^2 F_L}{\partial \lambda^2} \right) (x_L, y_L, z_L, 0) < 0. \quad (\text{A3})$$

In the following, it will be shown that the assertion (A3) is always correct for the improved objective function  $F_{L2}$  (4). Equations A4 and A5 are the first and second derivatives of objective function  $F_{L2}$  with respect to  $\lambda$ .

$$\begin{aligned} \left( \frac{\partial}{\partial \lambda} F_{L2} \right) (x, y, z, \lambda) &= \sum_{i=1}^N [(x - a_i)^2 + (y - b_i)^2 \\ &\quad + (z - c_i)^2 + \lambda^2 - d_i^2] \lambda, \end{aligned} \quad (\text{A4})$$

$$\begin{aligned} \left( \frac{\partial^2}{\partial \lambda^2} F_{L2} \right) (x, y, z, \lambda) &= \sum_{i=1}^N [(x - a_i)^2 + (y - b_i)^2 \\ &\quad + (z - c_i)^2 + \lambda^2 - d_i^2] + 2N\lambda^2. \end{aligned} \quad (\text{A5})$$

At the local minimum  $L(x_L, y_L, z_L)$ ,

$$\begin{aligned} \left( \frac{\partial^2}{\partial \lambda^2} F_{L2} \right) (0, 0, 0, 0) &= \sum_{i=1}^N [a_i^2 + b_i^2 + c_i^2 - d_i^2] \\ &= \sum_{i=1}^N \varphi_i(0, 0, 0) = \\ &= x_G \sum_{i=1}^N [2a_i - x_G] = 2x_G \sum_{i=1}^N a_i - Nx_G^2. \end{aligned}$$

We want to show that  $\left( \frac{\partial^2}{\partial \lambda^2} F_{L2} \right) (x_L, y_L, z_L, 0) < 0$ ; hence, we have to prove the inequality (A6).

$$\begin{aligned} 2x_G \sum_{i=1}^N a_i - Nx_G^2 &< 0 \\ 2 \sum_{i=1}^N a_i &< Nx_G. \end{aligned} \quad (\text{A6})$$

In the next step, the condition at the local minimum is analyzed. The first derivative of objective function  $F_2$  (2) equates to (A7),

$$\begin{aligned} \left( \frac{\partial}{\partial x} F_2 \right) (x, y, z) &= \sum_{i=1}^N [(x - a_i)^2 + (y - b_i)^2 \\ &\quad + (z - c_i)^2 - d_i^2] (x - a_i) = \\ &= \sum_{i=1}^N \varphi_i(x, y, z) (x - a_i), \end{aligned} \quad (\text{A7})$$

in combination with (A1), the first derivative becomes (A8).

$$\begin{aligned} \left( \frac{\partial}{\partial x} F_2 \right) (0, 0, 0) &= \sum_{i=1}^N \varphi_i(0, 0, 0) (-a_i) = \\ &= \sum_{i=1}^N x_G [2a_i - x_G] (-a_i) = \\ &= \left[ x_G^2 \sum_{i=1}^N a_i - 2x_G \sum_{i=1}^N a_i^2 \right]. \end{aligned} \quad (\text{A8})$$

At the local minimum  $L(x_L, y_L, z_L)$ , the first derivative of objective function  $F_2$  is equal to zero.

$$\begin{aligned} x_G^2 \sum_{i=1}^N a_i - 2x_G \sum_{i=1}^N a_i^2 &= 0 \\ x_G \sum_{i=1}^N a_i &= 2 \sum_{i=1}^N a_i^2. \end{aligned} \quad (\text{A9})$$

This leads to  $\sum_{i=1}^N a_i > 0$ . The objective function  $F_2$  has a higher result at the local minimum compared with the global minimum. It is assumed that the objective functions have no errors; therefore, the result of  $F_2$  at the global minimum must be zero.

$$F_2(0, 0, 0) > F_2(x_G, 0, 0) = 0, \quad (\text{A10})$$

$$\begin{aligned} x_G^2 \sum_{i=1}^N (2a_i - x_G)^2 &> 0 \\ \sum_{i=1}^N (2a_i - x_G)^2 &> 0 \\ 4 \sum_{i=1}^N a_i^2 - 4x_G \sum_{i=1}^N a_i + Nx_G^2 &> 0 \end{aligned} \quad (\text{A11})$$

$$4x_G \sum_{i=1}^N a_i < 4 \sum_{i=1}^N a_i^2 + Nx_G^2. \quad (\text{A12})$$

The term  $F_2(0,0,0)$  of (A10) is replaced by (A2). Equation A11 can be converted to A12. Combined with (A9), the new inequality equates to A13.

$$\begin{aligned} 8 \sum_{i=1}^N a_i^2 &< 4 \sum_{i=1}^N a_i^2 + Nx_G^2 \\ 4 \sum_{i=1}^N a_i^2 &< Nx_G^2. \end{aligned} \quad (\text{A13})$$

## A.2 | Proof by Cauchy-Bunyakovsky-Schwarz inequality

The final step of the proof for the assertion requires the Cauchy-Bunyakovsky-Schwarz inequality<sup>35</sup> for  $\mathbb{R}^N$ .

Here, it is desired to prove that  $2\sum_{i=1}^N a_i < Nx_G$ .

The Cauchy-Bunyakovsky-Schwarz inequality states that  $|\langle \vec{x}, \vec{y} \rangle| \leq \|\vec{x}\| \cdot \|\vec{y}\|$ . In our case, the vectors are the following:

$$\vec{x} = \begin{pmatrix} 1 \\ \vdots \\ 1 \end{pmatrix} \text{ and } \vec{y} = \begin{pmatrix} a_1 \\ \vdots \\ a_n \end{pmatrix}.$$

Therefore, the left term  $2\sum_{i=1}^N a_i$  of (A6) must be less than or equal to  $2\sqrt{N}\sqrt{\sum_{i=1}^N a_i^2}$ .

$$2 \sum_{i=1}^N a_i \leq 2\sqrt{N} \sqrt{\sum_{i=1}^N a_i^2}. \quad (\text{A14})$$

From (A13), it is known that  $\sum_{i=1}^N (a_i)^2 < \frac{1}{4}N \cdot (x_G)^2$ ; therefore, the right side of (A14) can be written as  $2\sqrt{N}\sqrt{\frac{1}{4}Nx_G^2}$ .

The inequality becomes

$$2 \sum_{i=1}^N a_i < 2\sqrt{N} \sqrt{\frac{1}{4}Nx_G^2} = Nx_G.$$

## A.3 | Possible constellations for the example

The coordinate system was described in Section A.1. We want to find base station constellations with a local minimum at  $x_L, y_L, z_L$  and a global minimum at  $x_G, y_G, z_G$ .

## A.4 | Analysis of the first derivative

The first derivative of objective function  $F_2$  has to be zero at the local minimum. This means

$$\left( \frac{\partial}{\partial x} F_2 \right) (0,0) = \sum_{i=1}^N [(a_i^2 - (x_G - a_i)^2) \cdot (-a_i)] = 0, \quad (\text{A15})$$

$$\left( \frac{\partial}{\partial y} F_2 \right) (0,0) = \sum_{i=1}^N [(a_i^2 - (x_G - a_i)^2) \cdot (-b_i)] = 0. \quad (\text{A16})$$

The simplest constellation that fulfills (A15) and (A16) is the following:

$$\begin{cases} [(a_i^2 - (x_G - a_i)^2) \cdot (-a_i)] = 0 & 1 \leq i \leq N \\ [(a_i^2 - (x_G - a_i)^2) \cdot (-b_i)] = 0 & 1 \leq i \leq N. \end{cases}$$

There are two obvious options that fulfill these equations. The first one is  $a_i = b_i = 0$ . The second one  $a_i = \frac{1}{2}x_G$  with any  $b_i$ . The number of base stations using the first and second options are denoted as  $S_1$  and  $S_2$ , respectively. Only sensible constellations are considered; therefore,  $S_1$  can only be one or zero.

## A.5 | Analysis of the second derivative

The second derivative of objective function  $F_2$  (2) must be positive at the local minimum. This means,

$$\left( \frac{\partial^2}{\partial x^2} F_2 \right) (0,0) = \sum_{i=1}^N [2a_i^2 + a_i^2 - (x_G - a_i)^2] > 0, \quad (\text{A17})$$

and

$$\left( \frac{\partial^2}{\partial y^2} F_2 \right) (0,0) = \sum_{i=1}^N [2b_i^2 - x_G^2 + 2a_i x_G] > 0. \quad (\text{A18})$$

Inserting (A15) into (A17) leads to the first condition.

$$\sum_{i=1}^N 3a_i > Nx_G. \quad (\text{A19})$$

The second and third conditions are obtained by inserting the options  $S_1$  and  $S_2$  into (A17) and (A18), respectively. Therefore, the second derivative of objective function  $F_2$  becomes

$$\left( \frac{\partial^2}{\partial x^2} F_2 \right) (0,0) = -S_1 x_G^2 + \frac{1}{2} S_2 x_G^2 > 0,$$

and

$$\left( \frac{\partial^2}{\partial y^2} F_2 \right) (0,0) = -S_1 x_G^2 + 2 \sum_{i=1}^{S_2} b_i^2 > 0.$$

All the conditions required for a local minimum at  $L(0,0)$  are listed in Table A1.

**TABLE A1** Conditions required for a local minimum at  $L(0, 0)$ 

	Conditions
1	$3 \sum_{i=1}^N a_i > Nx_G$
2	$0.5 \cdot S_2 > S_1$
3	$2 \sum_{i=1}^{S_2} b_i^2 > x_G^2 S_1$

**TABLE A2** Assumptions used for the example

Assumptions
$S_1 = 1$
$S_2 = 3$

**TABLE A3** Coordinates of object B

Base Stations $B_i$ With Index	X-Axis	Y-Axis
1	0	0
2	$0.5 \cdot x_G$	-2
3	$0.5 \cdot x_G$	1
4	$0.5 \cdot x_G$	3

## A.6 | Constellations used in the example

The assumptions used in the example and the coordinates of the base stations  $B_i$  can be found in Tables A2 and A3.